

# Operation of a High Gain Bidirectional DC-DC Converter for Photovoltaic On-grid Systems

Frederico José de Oliveira

Centro Federal de Educação Tecnológica de Minas Gerais  
EMAP SOLAR LTDA  
Belo Horizonte, Brazil  
frederico.oliveira@emapsolar.com.br

Elza Koeler de Barros Ribeiro

Dept. of Electrical Engineering  
Centro Federal de Educação Tecnológica de Minas Gerais  
Belo Horizonte, Brazil  
elzakoeler@des.cefetmg.br

Alex-Sander Amável Luiz

Dept. of Electrical Engineering  
Centro Federal de Educação Tecnológica de Minas Gerais  
Belo Horizonte, Brazil  
asal@des.cefetmg.br

Allan Fagner Cupertino

Dept. of Electrical Engineering  
Centro Federal de Educação Tecnológica de Minas Gerais  
Belo Horizonte, Brazil  
allan@des.cefetmg.br

**Abstract**—The aim of this paper is to present a dc-dc converter with high-stepping ratio for photovoltaic (PV) systems operating in parallel arrangement. The converter utilizes a resonant LC circuit to continue provide an increasing voltage at the output terminals by rotating the polarity of the capacitor using a thyristor based H-bridge. Compared with the existing converters, the proposed circuit reach higher voltage gains with low switching frequency using simple circuitry. It works efficiently with minimal switching loss even dealing with high currents. The prototype has shown the usefulness of the converter for low input voltage applications, mainly when a string of photovoltaic panels is connected in parallel, with the possibility to power in a commercial inverter.

**Keywords**—Resonant dc-dc converter; PV systems; high gain; bidirectional; operational dependency.

## I. INTRODUCTION

Renewable energy systems have been developed to provide part or full time powering for vehicles, houses, and industry. One of the most common sources of energy is the photovoltaic systems, which are composed by solar panels and a conversion unit that can be connected to energy storage devices or directly to the grid. Focusing on PV grid-tie utilities, a major problem is studied: the operational dependency of panels connected in series, also called strings. This paper aims to present a strategy for the issue by using an intermediate conversion unit with a high gain dc-dc converter.

It is well-known that solar panels have limited output voltage, which ranges from 12 to 48  $V_{dc}$ . Moreover, small scale solar inverters need an input voltage of at least 150  $V_{dc}$  to leave the stand-by mode. Therefore, the universal solution is the assembling of a string formed by a number of solar panels that can provide at least the minimum voltage required for the solar inverter start-up operation. The main disadvantage of this solution is the operational dependency of the panels in the

string, which means that if one panel of the string is out of service, the others connected in series will also be in open circuit. This effect will be the same in case of partial shading on one panel of a string, resulting in lower energy production. In this respect, the formation of large strings raises the losses and increases the parasitic capacitance to the ground, as the resistance and output voltage assume higher values for each panel connected in series [1].

To manage the operational dependency in a string, some techniques were developed, such as micro-inverters, PV balancers, and module-integrated-converters (MICs) [2-4]. Other possible way would be the connection of panels in parallel, so that each one could produce current independently. The solution's issue is that the output voltage is not enough to feed in a solar inverter.

An alternative approach for that would be an intermediate dc-dc conversion stage with a high voltage gain; therefore, being able to reach the input voltage requirement for the solar inverter. However, it has previously been difficult to transfer power with high voltage stepping, and, in particular, to obtain high boost levels. In this respect, conventional boost converters are not able to achieve voltage gains greater than 2-3 because of practical difficulties with diode recoveries, switching ratings, and the influence of parasitic elements when operating at extreme duty ratios [5,6]. Flyback or forward converters [5,7,8], are typically used to achieve higher voltage step ratios. However, such converters require an intermediate ac transformer which significantly increase the complexity and weight of the device. Further, whilst flyback and forward converters might be an acceptable solution for low power applications; however, they have numerous limitations and disadvantages at higher powers, such as high losses and switch stress.

---

This work was supported in part by PPGEL, CAPES and FAPEMIG.

When a voltage gain of around 10 is required, it has previously been found that it is most effective to use two stages of traditional boost converters [6], despite low efficiency and complexity. Recently, switched capacitor converters have been proposed, which achieve high voltage gain without the use of transformers [9]. However, these converters are modular, and become very complex, in addition to high losses if high-stepping ratios are required. In this respect, each module, which comprises one capacitor and a set of switches, only increases the output voltage by the value of the input voltage. Therefore, if high gains are needed, many modules are required.

Through the analysis of existing converters for low input voltage dc sources, it has been researched the necessary characteristics for the proposal of a high gain conversion unit that meets a set of requirements, such as low input voltage from panels connected in parallel, high-stepping ratios, bi-directionality for hybrid usage (energy storage and grid-tie systems), high efficiency, and capacity of dealing with high power flow. Therefore, a clever dc-dc converter has been found necessary to manage the power flow between energy sources (solar panels, electric grid), connected loads, and batteries. The block diagram of Fig. 1 shows the possible power flows for the arrangement cited.

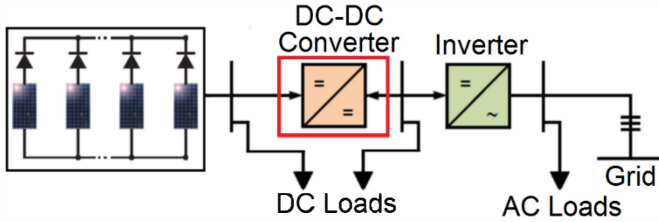


Fig. 1. Block diagram using full possibilities of the proposed converter.

The group of dc-dc converters that has been chosen is the resonant cluster, because of their known advantages, including high-stepping ratios, simplicity of circuit configuration, easiness of control, low switching losses, and low electromagnetic interference [10-12]. Based on these principles, it has been evaluated several dc-dc converters that were likely to meet the necessary requirements for the application, being chosen the bidirectional dc-dc resonant converter as shown in Fig. 2.

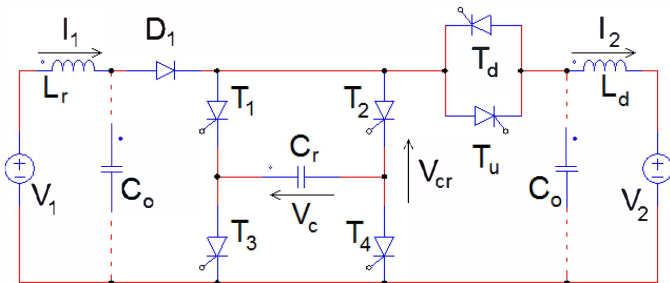


Fig. 2. Bidirectional DC-DC converter circuitry simulated on PSIM.

## II. RESONANT DC-DC CONVERTER

The resonant dc-dc power converter transfers power between low voltage terminals and high voltage terminals, with

a circuit comprising: an inductor and a capacitor across the low voltage terminals, the capacitor being provided in parallel with the high voltage terminals; a plurality of switches for switching the polarity of the capacitor in the circuit; and a controller for controlling the switching to repeatedly switch the polarity of the capacitor at a switching frequency  $f$ , such that, in use, and other than at the instant of switching, the switched capacitor produces an increasing voltage at the high voltage side of the inductor.

Thus, the dc-dc converter effectively utilizes a rotating capacitor in an LC circuit to achieve a constant permanent voltage increase at the high voltage side of the inductor. That is to say,

$$dV_{cr}/dt > 0 \quad (1)$$

where  $V_{cr}$  is the voltage produced by the switched capacitor at the high voltage side of the inductor. The firing of the thyristors changes the polarity of the capacitor  $C_r$  with a low switching frequency  $f_s$ . Consequently, the voltage gain is proportional to the speed that the capacitor polarity is reversed. The statement for the converter shown in Fig. 3, which will be the basis of all simulations presented in this paper, as no storage elements will be used primarily.

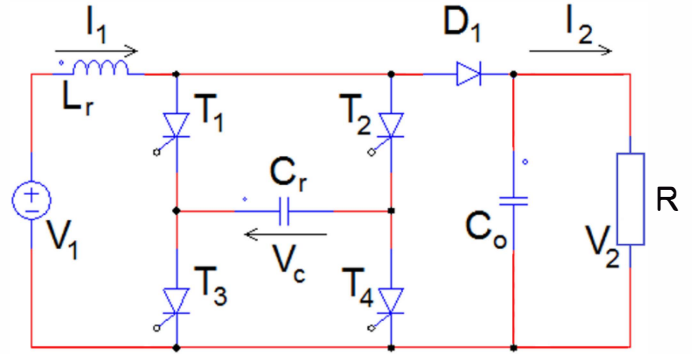


Fig. 3. DC-DC converter circuitry simulated on PSIM.

The constantly increasing voltage at the high voltage side of the inductor enables power to be transferred from the low voltage side of the circuit to the high voltage side of the circuit (step-up operation), and enables power to be transferred from the high voltage side of the circuit to the low voltage side of the circuit (step-down operation), as explained in more detail as follows.

The theoretical voltage achievable in boost or buck mode, under any non-zero and constant switching frequency (control signal), is infinity. Therefore, the output voltage of the circuit is only limited by the rating of the components. In particular, the circuit addresses the problem seen with conventional boost converters, of the output voltage level being directly linked with the magnitude of the control signal, such that operation becomes difficult as the control signal approaches extreme values. In this respect, the converter enables high voltage stepping ratios with minimal control action, and minimal sensitivity to the voltage level changes.

Moreover, the circuit does not require an iron-core transformer, and involves less complex electronic circuitry than conventional high gain converters, such as flyback or forward converters, and is thus simpler and cheaper to manufacture. In addition, the power circuit utilize thyristors and diodes, which are low cost, and have low losses and high power ratings. In contrast, previously known boost converters require switches with turn off ability, which have lower power ratings, higher losses and are high cost.

In step-up operation, the connecting device effectively allows the capacitor to be discharged to a high voltage load once per cycle, to transfer power from the low voltage side of the circuit to the high voltage load. In step-down operation, the connecting device connects the high voltage to the switched capacitor once per cycle to allow power to be transferred from the high voltage side to the low voltage side.

The capacitor may have a value  $C_r$  substantially equal to:

$$C_r = \frac{I_2}{2fV_1} \quad (2)$$

where  $I_2$  is the average current through the high voltage terminals,  $f$  is the switching frequency and  $V_1$ , is the voltage across the low voltage terminals. The capacitor may be switched at a switching frequency

$$f \leq 2f_c \quad (3)$$

where  $f_c$  is the natural frequency of the LC circuit constituted by the inductor and the capacitor. This results in discontinuous mode operation of the converter, which has intervals of zero current on the low voltage side. Discontinuous mode operation has the advantage of low switching losses, due to the fact that the initial and final current for each switching cycle is zero. In discontinuous mode operation, the inductor may have a value as shown in (4).

$$L_r = \frac{1}{\pi^2 f^2 C_r} \quad (4)$$

Where  $f$  is the switching frequency and  $C_r$  is the value of the capacitor. Alternatively, the capacitor may be switched at a switching frequency

$$f > 2f_0 \quad (5)$$

where  $f_0$  is the natural frequency of the LC circuit. This results in continuous mode operation of the converter. In continuous mode, the switching frequency is higher than in discontinuous mode, which results in lower input current ripple. Thus, a lower value capacitor than required for discontinuous mode operation may be employed, with consequent cost savings.

The principles of the proposed converter may be understood by analysis of the simple LC circuit which comprises an inductor  $L_r$  and a capacitor  $C_r$  connected in series, and driven by a voltage source  $V_1$ . The time domain

response of the current in the circuit,  $I_1$ , and the capacitor voltage  $V_{cr}$ , are given by (6) and (7).

$$I_1(t) = I_{10} \cos(\omega_0(t - t_0)) + ((V_1 - V_{cr0})/Z_0) \sin(\omega_0(t - t_0)) \quad (6)$$

$$V_{cr}(t) = (V_1 - V_{cr0}) \cos(\omega_0(t - t_0)) + Z_0 I_{10} \sin(\omega_0(t - t_0)) \quad (7)$$

where  $t$  is time,  $t_0$  is the initial time,  $I_{10}$  is the initial value of  $I_1$ , and  $\omega_0$  is the natural frequency of the LC circuit,  $V_1$  is the input voltage,  $V_{cr0}$  is the initial voltage of the capacitor, and  $Z_0$  is the natural impedance of the LC circuit. From (6), it is calculated the first derivative of the voltage with respect to time, as shown in (8).

$$\frac{dV_{cr}}{dt} = \omega_0(V_1 - V_{cr0}) \sin(\omega_0(t - t_0)) + \omega_0 Z_0 I_{10} \cos(\omega_0(t - t_0)) \quad (8)$$

By the analysis of (8), it can be concluded the conditions 1 and 2 respectively:

$$dV_{cr}/dt > 0, \text{ where } V_{cr0} < V_1, \text{ and } 0 < \omega_0 t < \pi \quad (9)$$

It has been established that condition 1 can be satisfied by rotating the capacitor  $C_r$  such that it changes polarity in the circuit when the capacitor voltage exceeds  $-V_1$ , and before it reaches its peak.

The capacitor must be rotated at a frequency of  $\omega$  as stated as condition 3 in (10)

$$\omega = 2\pi f > 2\omega_0 \quad (10)$$

i.e., switched in less than half the natural cycle, if the current  $I_1$ , is required to be continuous. In cases where the source  $V_1$  cannot tolerate a large ripple current, the inductor size can be increased, the operating frequency can be increased by using a smaller capacitor, or an additional input LC filter may be employed. From (8), it can also be concluded that the magnitude of  $dV_{cr}/dt$  (i.e., the slope of voltage increase) is directly proportional to both the natural frequency of the circuit,  $\omega_0$ , and  $V_{cr} - V_{cr0}$ . Thus, the higher the natural frequency of the circuit, the steeper the voltage rise. This in turn will raise the lower limit for the switching frequency (from condition 3).

With this arrangement, the polarity of the capacitor  $C_r$  in the circuit can be changed by firing switches  $T_1$  and  $T_4$  followed by switches  $T_2$  and  $T_3$ . The capacitor can thus be rotated in the circuit by alternately firing switches  $T_1$  and  $T_4$ , together, and  $T_2$  and  $T_3$  together. In this way, the capacitor always stays connected in parallel with the high voltage connection. However, the polarity of the capacitor repeatedly reverses. This principle is different from the switched capacitor converters [9], in which the capacitors are sequentially connected in series with the high voltage load. The firing of the switches  $T_1$  to  $T_4$  is at 50% duty cycle (equal conduction

interval for the  $T_1/T_4$  pair as for the  $T_2/T_3$  pair) and the frequency of rotation is the external control signal.

The commutation of capacitor current from one converter leg to the other is always assured. This means that the converter naturally extinguishes thyristor current. For example, by firing  $T_1$ , the input current  $I_1$ , is transferred from  $T_2$  to  $T_1$  since  $T_1$  provides lower cathode voltage and a lower resistance current path. The high voltage side capacitor voltage  $V_2$  is balanced by the diode current and the load current  $I_2$  as follows:

$$V_2 = (1/C_o) \int_0^{2\pi/\omega} (I_{d1} - I_1) dt \quad (11)$$

Equation (11) considers the integration over one full cycle, and implies averaging, because the diode current  $I_{d1}$  will be discontinuous. Diode  $D_1$  could potentially be replaced by a further thyristor in order to improve fault tolerance, in particular, tolerance to faults on the high-voltage side.

Fig. 4 shows a simplified schematic for a controller for controlling the switching of the circuit of Fig. 2. The controller comprises a primary feedback PI regulator which controls the output voltage  $V_2$ . Alternatively, the output current  $I_2$  or the input current  $I_1$ , or power, or some other variable could be controlled, depending on the application.

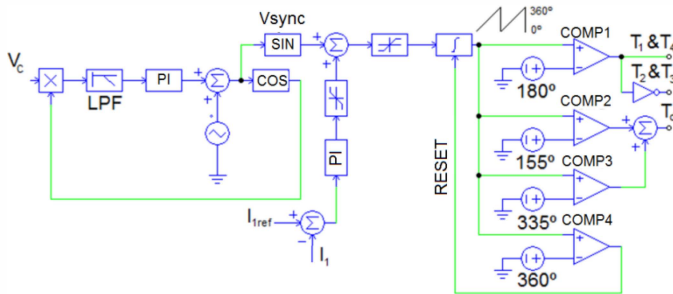


Fig. 4. Control circuit for step-up and step-down operations.

The controller also comprises a phase locked loop (PLL), which aids in synchronizing the firing of switches  $T_1$  to  $T_4$  with the capacitor voltage. The PLL improves stability at low operating frequencies, where time intervals between rotations are long. Where a PLL is required, it should have voltage magnitude compensation which could resemble that proposed in [6]. Fig. 5 shows the control signal during step-up operation and switching signal which increases the switching frequency as required to reach controlled variable in the control loop.

### III. SIMULATION PROCEDURES

Table 1 shows the size of each component used in simulations before the utilization of PV panels. Fig. 6 and Fig. 7 illustrate details of the PSIM simulation of the converter of Fig. 2 under very light loading. From Fig. 5 and 6 it can be seen that  $V_{cr}$  has a permanently increasing saw-tooth waveform, which is clipped as it reaches the level of  $V_2$ . The diode  $D_1$  discharges  $V_{cr}$  to the output capacitor once per cycle. In every cycle, there is an increase in the peak value of  $V_{cr}$ . This increase is identified as  $\Delta V_{cr}$ .

TABLE I. SYSTEM DATA

$C_r$	$L_r$	$C_o$	$R_2$	$V_1$	$L_d$
20 $\mu$ F	0.05H	50 $\mu$ F	1330 $\Omega^a$	12V <sub>dc</sub>	1mH

<sup>a</sup> Used for step-up operation as load resistance.

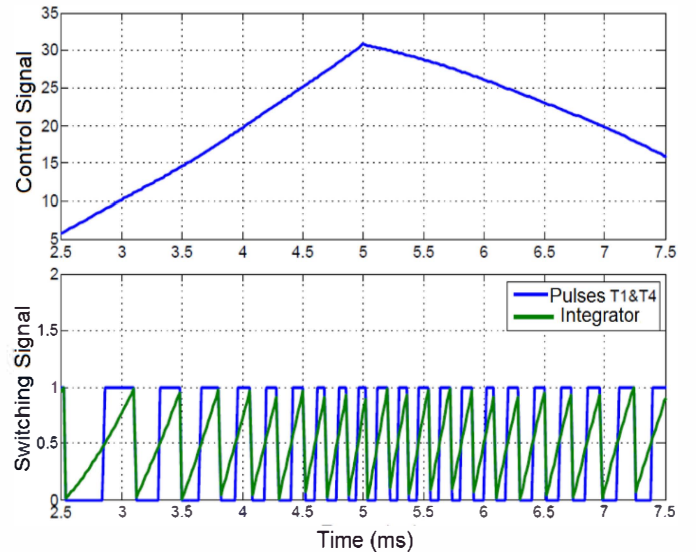


Fig. 5. Control and switching signal during step-up operation.

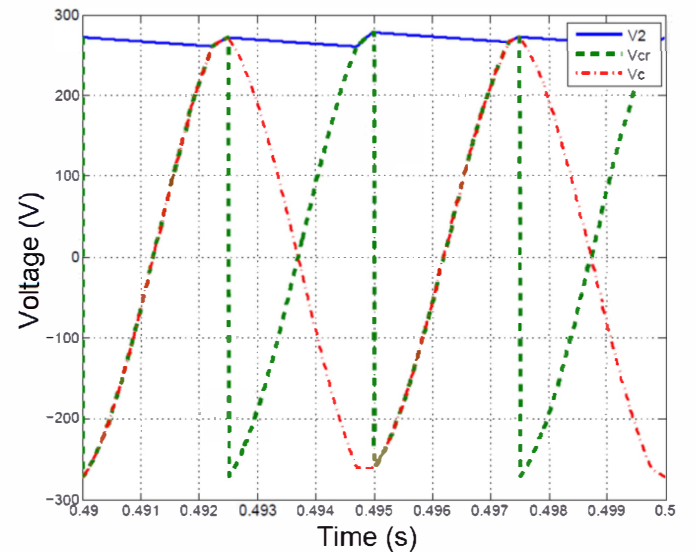


Fig. 6. Steady state operation with a 12V<sub>dc</sub> voltage source.

With reference to Fig. 6, the input current  $I_1$ , has a positive average value with some ripple which is proportional to the switching frequency, the inductor size and the loading. The current  $I_1$ , is positive, and, when multiplied by the positive voltage  $V_1$ , gives the electrical power taken by the converter input stage. This power is transferred to the switched capacitor and results in the peak voltage  $V_{cr}$  increase in each cycle.

In the test system illustrated in Fig.7, the current  $I_1$ , is continuous. However, at lower switching frequencies, the current  $I_1$ , will become discontinuous. In such cases, the

current  $I_1$ , will start from zero and will have full half-cycle. It will then end at zero and remain at zero until the next switching instant. Current  $I_1$ , cannot become negative because of the connection of the four switches  $T_1$  to  $T_4$ , and the diode  $D_1$ . The high voltage diode current  $I_{d1}$  has conducting intervals where the conduction interval length and the current magnitude depend on the voltage stepping ratio, the size of the output capacitor and the loading. The diode  $D_1$  has soft on-switching since it naturally turns on when the  $V_{cr}$  voltage exceeds the  $V_2$  voltage.

This is a significant advantage because similar diodes employed in previously known boost converters have hard on-switching. If the diode current gradient is of concern, it can be reduced by locating a small inductor in series with  $D_1$ .

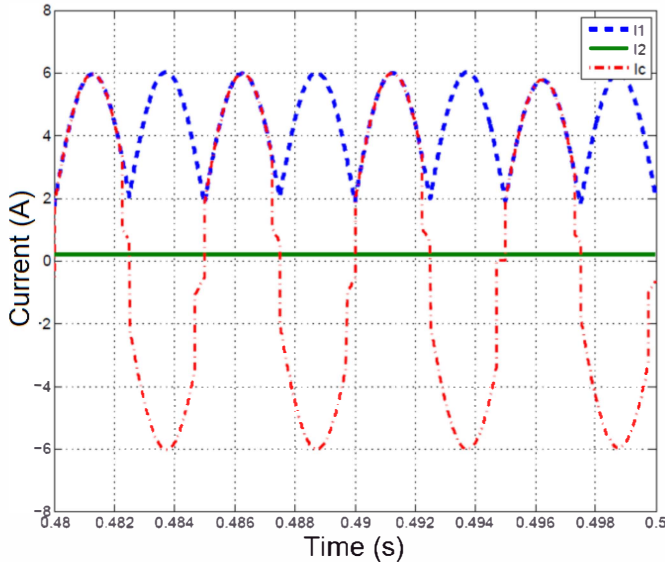


Fig. 7. Continuous conduction mode using light load.

In respect to the step-down operation, the pair of thyristor switches  $T_u$  and  $T_d$  connected together in parallel to control the power flow between the low and high voltage sides. Further, a small inductor  $L_d$  is connected in series with the cited thyristors. In the case of step-up operation, thyristor  $T_u$ , is permanently on and  $T_d$  is permanently off. In step-down mode, thyristor  $T_u$  is off and thyristor  $T_d$  is fired towards the end of voltage rise period, as indicated in the control system for the converter illustrated in Fig. 2.

The firing instant for  $T_d$  is given 25 degrees before the capacitor rotation, which is fired at 155 and 335 degrees. However, the phase angle at which the thyristor  $T_d$  is fired will depend on the practical application, and can be adapted. If the firing is later, i.e., closer to 180 and 360 degrees, the voltage stress on the thyristors is reduced, but the safe thyristor turning-off might be endangered. The thyristor  $T_d$  should switch off before the next capacitor rotation. This is achieved by the small inductor  $L_d$ , which creates resonant turn off with the capacitor  $C_r$ . The use of a single thyristor  $T_d$  is the simplest method for connecting the capacitor  $C_r$  with the high voltage terminals in step down mode.

An approximate value for the inductance of the inductor  $L_d$  is given by (12).

$$L_d \sim L_r/50 \quad (12)$$

This gives  $\sim 25$  degrees half period for  $L_d - C_r$ , on the main  $L_r C_r$  cycle (for operation at the border of discontinuous mode). With this interval, the current through the inductor extinguishes before the next firing of main switches  $T_1$  to  $T_4$ . Table 2 summarizes the signs of the input and output variables in the step-up and step-down operating modes.

TABLE II. VARIABLES FOR OPERATING MODES

Mode	$V_1$	$I_1$	$V_2$	$I_2$
Step-up	+	+	+	+
Step-down	-	+	+	-

Fig. 8 gives details of the simulation of the step-down operation of the bidirectional converter, using the test system data given in Table 1 and a high voltage source of  $300V_{dc}$ . As stated before, the main switches,  $T_1$  to  $T_4$ , are operated in the same fashion as with the step-up operation described in relation to the converter of Fig. 2. At the end of each capacitor voltage rise, the thyristor  $T_d$  is fired to enable power transfer from the high-voltage source. The capacitor current  $I_c$  peaks are higher with the step-down operation. However, the average capacitor current does not change significantly, which is important for switch ratings.

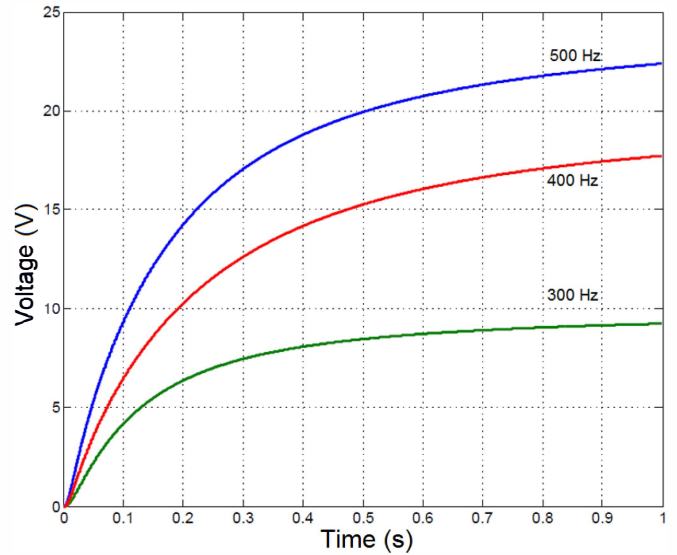


Fig. 8. Step-down operation using a  $300 V_{dc}$  voltage source at the output.

Considering the step-up operation, Fig. 9 gives the test results for an unloaded converter and a constant frequency operation. It can be seen from Fig. 8 that, at constant frequency, the output voltage  $V_2$ , initially increases linearly with time, and that gains of over 40 are achievable, as the input voltage of  $12 V_{dc}$  is used. This confirms the theoretical conclusions of positive  $\Delta V_{cr}$  in each step. It can also be seen that the rate of voltage increase decreases at higher output

voltages. This is the result of the increased losses and, in particular, switching losses.

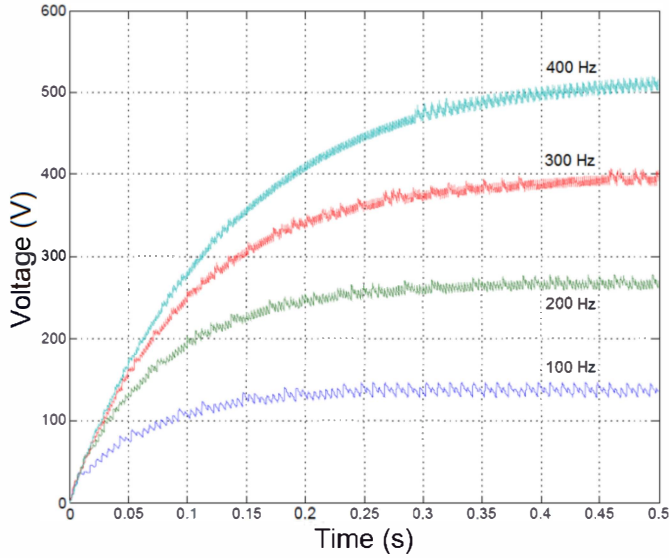


Fig. 9. Voltage response on step-up operation using a 12 V<sub>dc</sub> source.

Fig.11a and Fig. 11b demonstrate the responses for severe variations in the input voltage, load resistance, and voltage set point as shown in Fig. 10a to Fig. 10c. The high voltage  $V_2$  is controlled in a PI feedback loop. Since the high-power grid is undisturbed under low voltage side faults, this converter is convenient for high power applications.

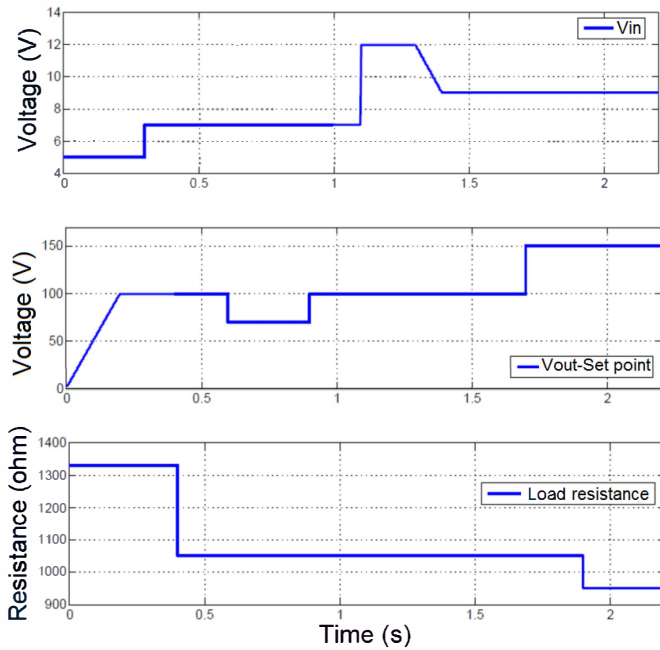


Fig. 10. (a) Input voltage variations for dynamic simulation of the converter on PSIM; (b) Input data for control circuit using different set points; (c) Variations in the load resistance during simulations.

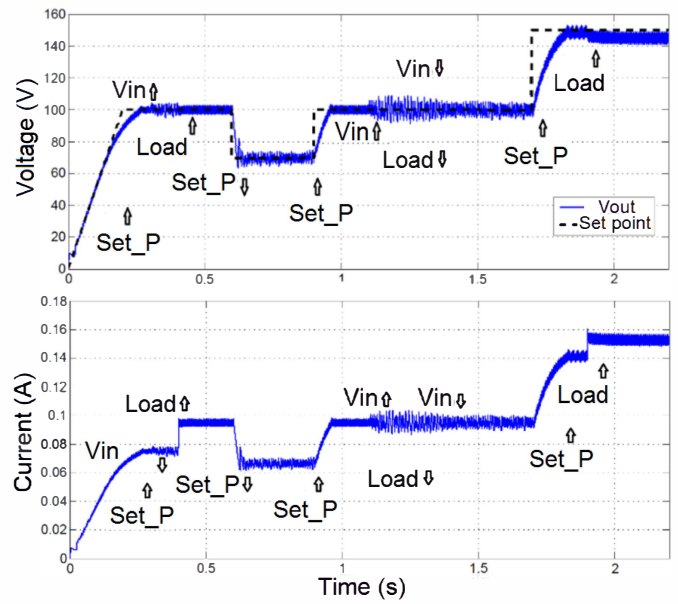


Fig. 11. (a) Voltage response based on input data presented; (b) Current response for a output voltage control loop as cited.

Faults on the high voltage side are also well tolerated and generally not propagated to the low voltage network. For transient faults which do not reduce  $V_2$  below the level of  $V_1$ , the converter simply recovers, as with the low voltage faults. If the fault reduces the voltage  $V_2$  below the value of  $V_1$  (which is less likely) then there is potential for  $V_1$  discharge in the fault, and control action is required. However a discharge of  $V_1$  can be avoided by simply turning off thyristor  $T_u$ , i.e., not firing  $T_u$  at the next firing instant. As a result of the transient simulations, Fig. 12 shows the efficiency of the converter under stressful conditions of load and high voltage stepping ratios.

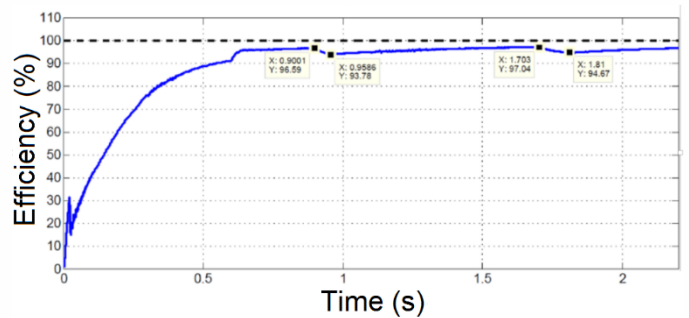


Fig. 12. Efficiency analysis based on input data provided.

#### IV. DC-DC CONVERTER FOR PV SYSTEMS

For complete evaluation of the photovoltaic conversion unit, a prototype of systems has been built to make the grid connection. The entire system is formed by a synchronization unit, maximum power point tracking (MPPT) control system, voltage source three-phase inverter, and three-phase current feedback loop based on PI (Proportional and Integral) controllers, as shown in Fig. 13.

For the synchronization system, the synchronous reference frame PLL is being used and applied to a three-phase current

control loop with PI based control: one PI controller for active and one for reactive power. To obtain the maximum efficiency of the panels, the Perturb & Observe and Incremental Conductance MPPT techniques have been implemented digitally. First tests have found the superiority of the incremental conductance method, achieving a performance of 98.5% when tracking the voltage and current of solar panels at the maximum power point.

As stated before, a three-phase voltage source inverter based on MOSFETs switches has been also built, and two switching algorithms are tested: sinusoidal pulse width modulation (SPWM) and space vector modulation (SVPWM). As expected, the SVPWM technique presented better output waveforms, with total harmonic distortion as low as 1.7% at a switching frequency of 15 kHz.

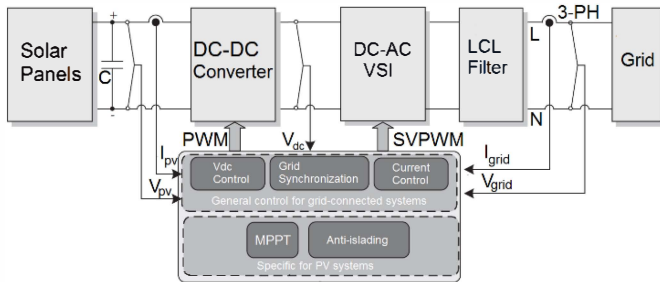


Fig. 13. Block diagram of a complete conversion unit for PV systems.

After the assembling of all subsystems on the software PSIM, a PV system is tested using 100 solar panels connected in parallel with 26 kWp. It was utilized the model KB260-6BCA from the manufacturer Kyocera. The string is designed at the normal operational conditions ( $800 \text{ W/m}^2$  and 20 degrees). In this case, each panel would produce 187 W at 27.47 V. Fig. 14 shows the output voltage and current of the dc-dc converter operating the PV systems specified.

The rated voltage gain utilized is considered low for the application; as a result, the voltage ripple is increased considerably. The average output power is 18.24 kW, achieving 98.4% for the dc-dc converter efficiency. In this respect, the high efficiency is due to the switching frequency below 200 Hz, as the voltage gain imposed is approximately 11. For higher output voltages, the voltage ripple would be lower and the system efficiency would also decrease slightly, as the switching frequency increases.

The inverter output power was 18.09 kW, which represents an overall efficiency of 97.5%. The inverter operation is set to provide a unitary power factor. For this case, the average output power of the dc-dc converter is connected to the active power reference of the current control loop of the inverter. The reactive power reference terminal had its terminals grounded. To demonstrate the quality of the current waveform, Fig. 15 shows the three-phase output current at the connection interface with the grid.

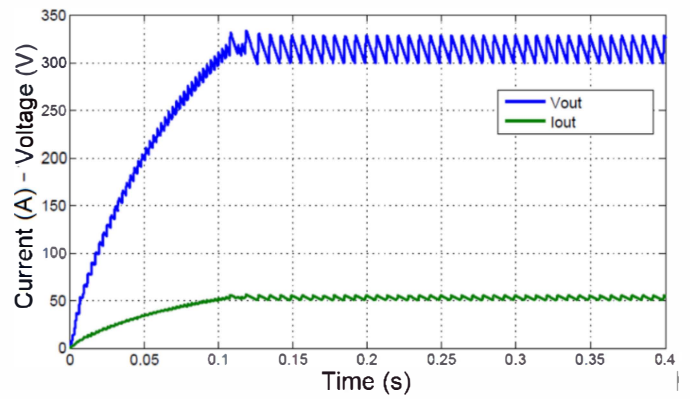


Fig. 14. Converter output current and voltage.

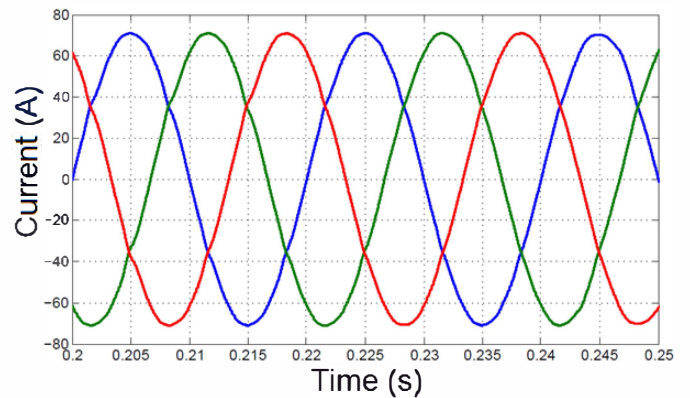


Fig. 15. Output current of the voltage source inverter.

The dc-dc converter was built for laboratory testing, as shown in Fig. 16, and it has been tested with lower input power for now. The printed circuit board is made using the software Proteus, with two layers as the switching drivers are built on the board. The entire system is being assembled to evaluate the performance of the connection and the overall efficiency while using the circuit of Fig. 2 for low input voltage applications.

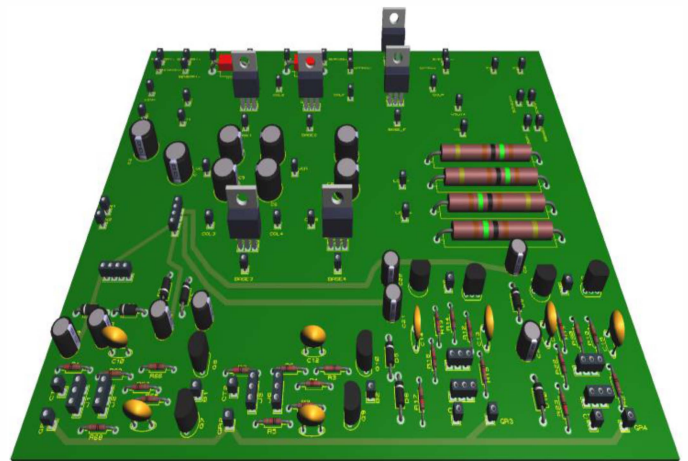


Fig. 16. Converter printed circuit board.

The plurality of switches are being changed to evaluate the performance with different typologies of drivers and modulators. It has been found that power BJTs can increase the overall efficiency of the system. The disadvantage is the complexity of base drivers, which can easily unbalance the H-bridge.

As the study continues on, the next steps of analysis are:

- Simulation of the conversion unit with a dc bus bar in between the panels and the dc-dc converter. The formation of this structure will allow the bidirectional operation to operate in a hybrid mode, by using the power flow from the dc-dc converter to the grid, and from the grid to energy storage systems, as the dc-dc converter can operate as a buck converter. The first tests are indicating the utilization of the 12 V dc bus bar for battery charging; however, this solution still requires further testing. To build this topology, a rectifier would be added to the conversion unit, in case of using the grid to power dc loads or charge batteries.
- Continuation of the laboratory tests involving the dc-dc converter prototype. The converter has been tested using fixed dc power supply equipment, and a MPPT is being implemented digitally for the usage in a solar panel. It is expected at least 98.5% of efficiency in the maximum power point algorithm.

## V. CONCLUSIONS

The simulation tests described focus on the low-frequency range of 150-500 Hz, which implies small switching losses. However, a converter which embodies the present circuitry could be made to operate at much higher frequencies. In this case, the passive components would be smaller, as required for high power density applications.

The proposed resonant dc-dc converter can be used in electronics systems for connection of low-voltage dc sources to dc networks at various power levels. They can also be used with switched-mode power supplies which require widely varying dc voltage levels, as with modern consumer electronics. They could also replace conventional high-gain dc-dc converters in many low power applications. Converters which embody the proposed converter also provide opportunities for better utilization of dc electrical networks. In mixed ac-dc electrical systems, converters which embody the present invention can also be used as an alternative for conventional iron-core transformers

## REFERENCES

[1] Venu Sonti, Sachin Jain, Subhashish Bhattacharya, "Analysis of the Modulation Strategy for the Minimization of the Leakage Current in the PV Grid-Connected Cascaded Multilevel Inverter", *Power Electronics IEEE Transactions on*, vol. 32, pp. 1156-1169, 2017, ISSN 0885-8993.

[2] B. Sahan, A. N. Vergara, N. Henze, A. Engler, P. Zacharias, "A single-stage PV module integrated converter based on a low-power current-source inverter", *IEEE Trans. Ind. Electron.*, vol. 55, no. 7, pp. 2602-2609, Jul. 2008.

[3] G. R. Walker, J. C. Pierce, "Photovoltaic dc-dc module integrated converter for novel cascaded and bypass grid connection topologies—Design and optimisation", *Proc. IEEE PESC*, pp. 3094-3100, 2006.

[4] C. D. Townsend, G. Mirzaeva, G. C. Goodwin, G. Konstantinou, J. Pou, "Fractionally-rated DC-DC stages for use in multilevel cascaded converter utility-scale battery energy storage systems", *Power Electronics Conference (SPEC) IEEE Annual Southern*, pp. 1-6, 2016.

[5] N Mohan, T M Undeland, W P Robbins, "Power Electronics Converters, Applications and Design," John Wiley & Sons, 1995.

[6] L Huber, M Jovanovic "A design approach for server power supplies for networking applications" *Proceedings IEEE applied power electronics conference, APEC '00* vol. 2, February 2000, pp 1163-1169.

[7] R J Wai, RY Duan, "High step-up converter with coupled inductor" *IEEE Transactions on Power Electronics*, vol 20, no 5, September 2005, pp 1025-1035.

[8] Q Zhao, F C Lee "High Efficiency, high step up DC-DC converters" *IEEE Transactions on Power Electronics*, Vol 18, no 1, January 2003, pp 65-73.

[9] Abutbul, et al "Step-up Switching Mode Converter With High Voltage Gain Using a Switched-Capacitor Circuit" *IEEE Transactions On Circuit and Systems-I* Vol. 50, no 8, August 2003, pp 1098-2002.

[10] W. Chen, A. Huang, C. Li et al., "Analysis and comparison of medium voltage high power DC/DC converters for offshore wind energy systems", *IEEE Trans. Power Electron.*, vol. 28, no. 4, pp. 2014-2023, 2013.

[11] A. Parastar, A. Gandomkar, M. Jin, J. Seok, "High power solid-state step-up resonant Marx modulator with continuous output current for offshore wind energy systems", *Proc. IEEE ECCE*, pp. 1709-1716, 2013.

[12] D K Choi, et al "A novel power conversion circuit for cost effective battery fuel cell hybrid system" *Elsevier Journal of Power Sources*, Vol 152, (2005), pp 245-255.